JOURNAL OF VIROLOGY, May 2010, p. 4302–4310 Vol. 84, No. 9
0022-538X/10/$12.00 doi:10.1128/JVI.02284-09

Viral Dynamics during Primary Simian Immunodeficiency Virus Infection: Effect of Time-Dependent Virus Infectivity▽

Naveen K. Vaidya,[1] Ruy M. Ribeiro,[1] Christopher J. Miller,[2] and Alan S. Perelson[1]*

Theoretical Biology and Biophysics Group, MS K710, Los Alamos National Laboratory, Los Alamos, New Mexico 87545,[1] and California National Primate Research Center, University of California, Davis, California 95616[2]

Received 28 October 2009/Accepted 3 February 2010

A recent experiment involving simian immunodeficiency virus (SIV) infection of macaques revealed that the infectivity of this virus decreased over the first few months of infection. Based on this observation, we introduce a viral dynamic model in which viral infectivity varies over time. The model is fit to viral load data from eight (donor) monkeys infected by intravaginal inoculation of SIVmac251, three monkeys infected by intravenous inoculation of virus isolated from the donors during the ramp-up phase of acute infection, and three monkeys infected by intravenous inoculation of virus isolated at the viral set-point. Although we only analyze data from 14 monkeys, the new model with time-dependent infectivity seems to fit the data significantly better than a widely used model with constant infectivity ($P = 2.44 \times 10^{-11}$). Our results indicate that plasma virus infectivity on average decays ~8-fold (95% confidence interval [CI] = 5.1 to 10.3) over the course of acute infection, with the decay occurring exponentially with an average rate of 0.28 day^{-1} (95% CI = 0.14 to 0.42 day^{-1}). The decay rate in set point plasma virus recipient animals is ~16 times slower than in ramp-up plasma virus recipient animals and ~6 times slower than in donor animals. Throughout acute infection up to the set-point, the infection rate is higher in ramp-up plasma virus recipient animals than in set-point plasma virus recipient animals. These results show that the infectivity depends upon the source of viral infection.

During primary human immunodeficiency virus type 1 (HIV-1) infection, the number of virus particles in plasma increases rapidly, reaches a peak, and then declines until it reaches a set-point level (i.e., a quasi-steady state) (9, 43). During the first 1 to 3 weeks of a typical HIV infection the viral load remains below the limit of detection of conventional assays (12). This period, known as the eclipse phase, is followed by a 2- to 4-week ramp-up period, during which rapid (exponential) viral replication takes place, resulting in high plasma viral RNA levels and significant depletion of $CCR5^+$ $CD4^+$ T cells (12, 24, 31, 47).

A recent experiment indicates that the infectivity of SIV changes over time during primary infection (26). Ma et al. (26) infected macaques with SIV isolated either during ramp-up or at set-point. They found that early-stage plasma containing 20 SIV RNA copies could successfully infect animals, while with set-point plasma ~1,500 SIV RNA copies were needed to establish infection. As suggested by Ma et al. (26), the highly infectious virus during the early phase compared to the chronic phase could be due to (i) insufficient rounds of replication during the early phase to produce enough noninfectious viral genomes; (ii) coating of the set-point phase plasma virions with antibodies that interfere with infectivity; and/or (iii) efficient elimination during early-phase infection of less-infectious genomes. Preliminary data comparing the ratio of the 50% tissue culture infectious dose ($TCID_{50}$) with HIV RNA copy number also suggests a decrease of virus infectivity over time during primary infection in HIV-1-infected patients (David Montefiori, Duke University School of Medicine, unpublished data).

Primary simian immunodeficiency virus (SIV)/HIV-1 infection has been studied both experimentally and via modeling (3, 6, 8, 13, 15, 25, 32, 33, 36, 37, 39, 44). However, none of the within-host models in these studies has considered the time variation of virus infectivity. The main objective of the present study was to evaluate the effect of time-dependent virus infectivity on SIV/HIV-1 dynamics (as observed in reference 26).

We introduce a viral dynamic model with a particular function describing the time-dependent infectivity. We fit the model to viral load data obtained from eight monkeys infected by intravaginal inoculation of SIVmac251 (the donor animals), three monkeys infected by intravenous inoculation of ramp-up plasma virus from the donor monkeys, and three monkeys infected by intravenous inoculation of set-point plasma virus from the donors (26) and then estimated key parameters. Our model fits the data well, and the inclusion of a time-dependent infectivity was found to be statistically significant for 8 of 11 animals analyzed.

MATERIALS AND METHODS

Experimental data. In an experiment to analyze the infectivity of plasma at different time points after SIV infection (26), Ma et al. made pools of plasma containing virus collected during the ramp-up stage or set-point stage of infection from eight rhesus macaques (the donor monkeys) infected intravaginally by a cell-free stock of SIVmac251. They then used those two pools of plasma from different stages of infection to titrate the amount needed for subsequent intravenous infection of naive rhesus macaques (for further details, see reference 26). We model the kinetics of acute infection in these eight donor animals (25479, 25948, 29459, 29271, 27361, 29029, 26811, and 25908) and in six recipient animals (35036, 33815, 34373, 33952, 34846, and 36068) from (26). Three of the latter (35036, 33815, and 36068) were infected by intravenous inoculation of ramp-up plasma, while the other three (34373, 33952, and 34846) were infected by intravenous inoculation of set-point plasma. The median peak viral load was 7.5 (7.0 to 8.6) $\log_{10}$ viral RNA (vRNA) copies/ml in the donor animals and 7.9 (7.4 to

* Corresponding author. Mailing address: Theoretical Biology and Biophysics Group, MS K710, Los Alamos National Laboratory, Los Alamos, NM 87545. Phone: (505) 667-6829. Fax: (505) 665-3493. E-mail: asp@lanl.gov.

▽ Published ahead of print on 10 February 2010.

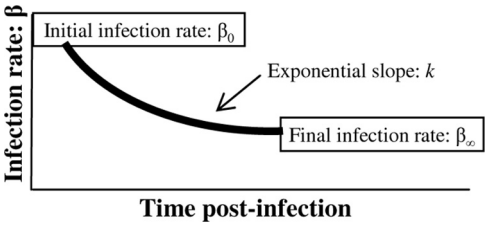

FIG. 1. Time-dependent infection rate β.

8.4) $\log_{10}$ vRNA copies/ml in the recipient animals. The set-point level to which the viral load declines after the peak varied widely among animals from 3.6 to 7.5 $\log_{10}$ vRNA copies/ml.

Viral dynamics model. The model developed in the present study generalizes the basic model of viral infection by incorporating time-dependent virus infectivity. The basic model, which consists of target cells ($CD4^+$ T cells), T, productively infected $CD4^+$ T cells, T^*, and free virus, V, has been widely used to describe the virus dynamics of SIV/HIV-1 primary infection (25, 33, 35, 36, 44). This basic model has been extended by incorporating an immune response, time delays and different classes of target cells (2, 8, 10, 32, 34). However, none of these previous models has included the effect of a time-dependent infection rate. The model we study is

$$\begin{aligned} \frac{dT}{dt} &= \lambda - dT - \beta(t)TV, & T(0) &= T_0 \\ \frac{dT^*}{dt} &= \beta(t)TV - \delta T^*, & T^*(0) &= T_0^* \\ \frac{dV}{dt} &= pT^* - cV, & V(0) &= V_0 \end{aligned} \tag{1}$$

where

$$\beta(t) = \beta_\infty + (\beta_0 - \beta_\infty)e^{-kt} \tag{2}$$

We assume that target cells are generated at a constant rate λ, have a per capita net loss rate d, which is the difference between loss from cell death and gain due to cell division, and become infected at a rate proportional to the product of target cell density and virus concentration with a time-dependent rate $\beta(t)$. The parameters δ, p, and c are the rate constants of infected cell loss, virus production by infected cells, and virus clearance, respectively.

Based on the experimental data in Ma et al. (26), we assume that the rate of virus infection $\beta(t)$ decays over time. The data are not sufficient to determine the exact form of $\beta(t)$. Here we assume a simple exponential decay in infectivity over time from the initial rate β_0 to the final set-point rate β_∞ with a decay rate k, as shown in Fig. 1. We shall show this exponential form provides a good fit to the available data and is convenient to study the properties related to viral dynamics during primary infection. We note that when $k = 0$, $\beta(t)$ is constant and equal to β_0, and thus we recover the basic model of virus dynamics.

Data fits and parameter estimation. We fitted the model, equation 1, to experimental data, assuming both constant and time-varying infectivity.

Stafford et al. (44) showed that for the model given by equation 1, one can only estimate the product pT_0 of the viral production rate, p, and the initial number of target cells, T_0, and not the individual quantities. Therefore, we estimate only one of them, in this case T_0. We fix p based on the work of Chen et al. (7), who estimated the SIV burst size *in vivo* in rhesus macaques as approximately 5×10^4 virions per infected cell. Because productively infected cells live about 1 day (29), we assume the viral production rate $p = 5 \times 10^4$ virions per day per infected cell. Assuming $CD4^+$ T cells were at equilibrium before infection, we set $\lambda = dT_0$, where T_0 is the initial number of target cells. Since the animals had not been previously infected by SIV, we set $T_0^* = 0$. Recent estimates show that the virion clearance rate constant during chronic infection in human varies between 9.1 and 36.0 day^{-1}, with an average of 23 day^{-1} (41). Moreover, results in acute infection of rhesus macaques indicate that SIV clearance from plasma is at least as fast (49). Thus, we take $c = 23$ day^{-1} as a minimal estimate, although other values could also be considered.

In the experiment by Ma et al. (26), 20 vRNA copies of ramp-up plasma were injected i.v. into recipient animals. A 70-kg man has about 15 liters of extracellular body water. The average weight of a macaque is ~10-fold less, which provides ~1,500 ml of extracellular body water in a macaque. Similarly, the plasma volume of a 7 kg macaque is ca. 10% of that of a 70 kg human, i.e., ~300 ml. Thus, upon injection the initial plasma viral load is 20 vRNA copies per 300 ml or 20 vRNA copies per 1,500 ml depending upon whether the virus distributes throughout only the plasma or the total extracellular body water before initiating infection. Studying both cases, we found that a change of V_0 from 20/300 vRNA per ml to 20/1,500 vRNA per ml did not produce any significant change in estimated parameters. Therefore, we assume the injected virus distributes in the plasma, and we present the results with $V_0 = 20/300$ vRNA per ml. To infect set-point plasma recipient animals, 1,500 vRNA copies were injected i.v. Thus, we take $V_0 = 1{,}500/300$ vRNA copies per ml for set-point plasma recipient animals. The donor animals were exposed to SIVmac251 by intravaginal inoculation. The exact number of vRNA copies that penetrated the vaginal mucosa and initiated infection is not known. However, a similar experiment (19) showed that in four of six animals infected intrarectally with SIVmac251 only a single virus variant initiated observable infection. Based on this information, we set $V_0 = 1/300$ vRNA copies per ml for donor animals. Recognizing that the initial infecting virus does not simply dilute into plasma, we have also studied the sensitivity of parameter estimates on V_0 by taking V_0 10- and 100-fold higher in the donor animals. Since one virion contains two vRNA copies, one might want to set $V_0 = 2/300$ copies/ml, but since two vRNAs in our model can infect two cells, we felt it more realistic to use $V_0 = 1/300$. Moreover, we found that $V_0 = 1/300$ or $2/300$ does not make any significant difference in the estimated parameters.

By keeping p, c, and V_0 fixed in each fit, we need to estimate six parameters β_0, β_∞, k, δ, d, and T_0 from the data of each of eight donor animals, three ramp-up plasma recipients, and three set-point plasma recipients. For both models (our model with time-dependent infectivity and the model with constant infectivity), we solved the system of ordinary differential equations (ODEs) numerically using a fourth-order Runge-Kutta in Berkeley Madonna (27). Using Madonna's "curve fitter" option, we obtain a set of initial parameter estimates. The curve fitting method uses nonlinear least-squares regression that minimizes the following sum of the squared residuals:

$$J(\beta_0, \beta_\infty, k, \delta, d, T_0) = \frac{1}{N}\sum_{i=1}^{N}[\log V(t_i) - \log \bar{V}(t_i)]^2 \tag{3}$$

Here, V and $\bar{V}$ are virus concentrations predicted by the model and those given by the experimental data, respectively. N is the total number of data points considered for fitting.

Using the set of parameters obtained from Madonna as initial guesses, we further fitted the data by using a more sophisticated subroutine, DNLS1, from the Common Los Alamos Software Library, which is based on a finite-difference, Levenberg-Marquardt algorithm for solving nonlinear least square problems and a more sophisticated ODE solver that uses an implicit Adam's method or, if the equations are stiff, Gear's method. For animal 34846, since only four data points are available, we fixed δ and d as obtained from Madonna's fit and estimated the remaining four parameters. Finally, for each best fit parameter estimate, we provide a 95% confidence interval (CI), which was computed from 500 bootstrap replicates (11).

Sensitivity analysis. For donor animals, viral RNA copies at the time of infection, V_0, were not known. To study the sensitivity of estimated parameters to the choice of V_0, we increased V_0 by 10-fold, making it 10/300 ml, and 100-fold, making it 100/300 ml, and in each case estimated all six remaining parameters for each of the eight donor animals.

Statistical analysis. To evaluate the statistical significance of the fits obtained with our model, with varying infectivity, versus those obtained with constant infectivity, we performed an F test (4). Our model and the simple model can be taken as nested models; when k and β_∞, the additional parameters in our model, are zero, we recover the simpler model. In fact, regardless of β_∞, when $k = 0$ in our model, we recover the model with constant infectivity. However, as we varied both parameters k and β_∞ in our fitting, we penalized our model by two extra parameters to obtain a more conservative comparison. As in reference 4, we calculate the F-ratio $= s_e^2/s_f^2$. Where s_e^2 is the difference between the residual mean square (RSS) of the two models divided by the number of additional parameters (i.e., two in our case). And s_f^2 is calculated by dividing the RSS of the varying-infectivity model by the difference between the number of data points and the number of free parameters. We then compare the ratio with an F distribution with the appropriate degrees of freedom. In addition to testing the new model for each macaque, we also tested whether it is better overall by summing the individual RSS and degrees of freedom for each animal and performing an F test based on this. Thus, we obtained a global P value for the improvement of the fit afforded by the model with time-varying infectivity.

TABLE 1. Time-dependent infectivity model: estimated parameter values[a]

Animal group[b]	T_0 (cells/μl)	β (10^{-8} ml/RNA/day)		β_0/β_∞
		β_0	β_∞	
Group 1				
25479	119.5 (71.7–551.2)	2.13 (0.33–3.99)	0.17 (0.004–0.48)	12.5
25948	20.4 (15.8–40.2)	13.27 (6.59–16.37)	1.41 (0.89–1.99)	9.4
29459	106.1 (97.0–118.1)	1.87 (1.66–2.57)	0.86 (0.48–1.13)	2.2
29271	100.5 (72.0–171.8)	2.44 (1.23–4.03)	0.17 (0.10–1.01)	14.3
27361	36.4 (27.7–43.0)	11.97 (10.59–14.77)	0.68 (0.54–0.87)	17.6
29029	64.7 (42.3–111.0)	4.28 (2.57–6.58)	0.43 (0.31–0.71)	9.9
26811	31.4 (10.8–129.1)	8.15 (1.61–24.7)	1.81 (0.51–4.09)	4.5
25908	38.0 (26.5–57.9)	5.22 (3.34–7.76)	0.76 (0.42–1.03)	6.9
Mean	64.6	6.17	0.79	9.7
Median	51.3	4.75	0.72	9.7
Group 2				
35036	79.8 (64.1–149.4)	4.65 (2.62–6.50)	0.94 (0.50–1.09)	4.9
33815	38.9 (30.3–49.1)	5.90 (3.43–6.75)	2.40 (1.70–2.85)	2.4
36068	25.7 (5.2–29.7)	6.54 (1.48–18.55)	3.84 (3.06–21.86)	1.7
Mean	48.1	6.0	2.39	3.0
Median	38.9	5.9	2.40	2.4
Group 3				
34373	62.0 (31.4–156.2)	2.10 (0.72–2.93)	0.20 (0.10–23.8)	10.5
33952	66.6 (57.0–78.1)	2.00 (1.74–2.33)	0.23 (0.06–0.31)	8.7
34846	31.2 (31.2–31.2)	3.20 (3.20–3.20)	1.16 (1.16–1.16)	2.7
Mean	53.3	2.4	0.53	7.3
Median	62.0	2.1	0.23	8.7
Overall mean	58.7 (41.7–75.6)	5.3 (3.34–7.18)	1.08 (0.53–1.61)	7.7 (5.1–10.3)
Overall median	50.4	4.47	0.81	7.8

[a] Estimated parameter values T_0, β_0, β_∞, k, δ, d, time T_h to reach the mid-value $(\beta_0 + \beta_\infty)/2$, sum of squared residuals (SSR), and the P value of the F-test for the eight donor animals, three ramp-up plasma recipient animals, and three set-point plasma recipient animals. Numbers in parentheses indicate the 95% CI.

[b] Group 1, donor animals, intravaginally infected; V_0 = 1 RNA copy per 300 ml; group 2, ramp-up plasma recipient animals, i.v. infected; V_0 = 20 RNA copies per 300 ml; group 3, set-point plasma recipient animals, i.v. infected; V_0 = 1,500 RNA copies per 300 ml.

RESULTS

Model-fit to the data. Estimated parameters along with their mean, median, and 95% confidence intervals are summarized in Tables 1 and 2 using the time-dependent infectivity model and the constant infectivity model, respectively. Using these estimated parameters, we plotted the viral load dynamics predicted by the models along with the data for each of the eight donor animals and the six recipient animals in Fig. 2 and 3, respectively. The predictions of our time-varying infectivity model (solid curve) agree well with the data (dot). Although the model with constant infectivity can also give reasonable fits (dashed curve), the dynamics predicted by the two models are quite different, particularly at early times. The model with time-dependent infectivity provides better fits to the data as indicated in Fig. 2 and 3 and as determined by the sum of squared residuals (SSR) given in Tables 1 and 2.

To evaluate the statistical significance of using a time-dependent infection rate rather than a constant infection rate, we performed an F-test (4) for seven donor animals (25479, 25948, 29271, 27361, 29029, 26811, and 25908), all three ramp-up plasma recipient animals, and one set-point plasma recipient animal (animal 33952). We did not consider donor animal 29459 and set-point plasma recipient animals 34373 and 34846 due to the lack of sufficient data to perform this test. We found that our model is statistically significant for 8 out of 11 cases (animals 25479, 25948, 27361, 29029, 26811, 35036, 33815, and 33952). For the remaining three animals (29271, 25908, and 36068) even though the SSR is less in our model, the improvement is not statistically significant (Tables 1 and 2). We also calculated a global P value (see Materials and Methods) comparing the fits of the two models for the entire set of 14 animals. We found $P = 2.44 \times 10^{-11}$, which indicates that the model with time-dependent infectivity is better overall.

Initial and set-point infectivity. The average initial and set-point viral infection rates were estimated to be β_0 = 5.3 (95% CI = 3.3 to 7.2; median, 4.5) $\times 10^{-8}$ ml RNA^{-1} day^{-1} and β_∞ = 1.1 (95% CI = 0.53 to 1.6; median, 0.81) $\times 10^{-8}$ ml RNA^{-1} day^{-1}, respectively. This shows that set-point plasma virus is less infectious than ramp-up plasma virus, supporting the experimental finding in Ma et al. (26). Calculating the ratio of β_0 to β_∞, we found that the ramp-up plasma virus has an infection rate that is 7.7 (95% CI = 5.1 to 10.3; median, 7.8) times greater than the set-point plasma virus. The model with constant infectivity provides an average infection rate of $\bar{\beta}$ = 4.8 (95% CI = 2.6 to 7.0; median, 3.5) $\times 10^{-8}$ ml RNA^{-1} day^{-1} (Table 2), which is slightly less than the initial infection rate in the varying-infectivity model but almost five times higher than the set-point infection rate.

Time-dependent infection rate. The infection rate, $\beta(t)$, decays from the initial infection rate to the set-point infection rate. Assuming that the decay is exponential, we found that the rate of decay in virus infectivity ranges from k = 0.03 day^{-1} (animal 33952) to k = 0.75 day^{-1} (animal 33815) with an average k = 0.28 (95% CI = 0.14 to 0.42; median, 0.16) day^{-1}.

TABLE 1—*Continued*

k (1/day)	δ (1/day)	*d* (1/day)	T_h (days)	SSR	*P* (F-test)
0.13 (0.03–0.62)	0.17 (0.09–0.56)	0.056 (0.021–0.297)	5.3	0.029	0.0113
0.16 (0.09–0.24)	0.56 (0.38–0.87)	0.047 (0.017–0.081)	4.3	0.031	0.0171
0.16 (0.09–0.45)	0.34 (0.31–0.41)	0.031 (0.025–0.051)	4.3	0.002	
0.12 (0.05–0.23)	0.27 (0.21–0.45)	0.017 (0.002–0.066)	5.8	0.005	0.0761
0.34 (0.27–0.44)	0.45 (0.35–0.55)	0.030 (0.019–0.079)	2.0	0.019	0.0071
0.20 (0.19–0.23)	0.41 (0.29–0.58)	0.054 (0.031–0.073)	3.5	0.0008	<0.0001
0.72 (0.16–1.84)	0.32 (0.15–0.87)	0.014 (0.004–0.032)	1.0	0.239	0.0439
0.07 (0.04–0.11)	0.61 (0.58–0.68)	0.047 (0.034–0.077)	9.9	0.024	0.1279
0.24	0.39	0.037	4.5		
0.16	0.37	0.039	4.3		
0.55 (0.35–1.24)	0.26 (0.23–0.30)	0.004 (0.003–0.006)	1.3	0.116	0.0029
0.75 (0.10–0.89)	0.20 (0.16–0.24)	0.009 (0.006–0.012)	0.9	0.033	0.0025
0.67 (0.20–1.11)	0.28 (0.21–0.39)	0.003 (0.001–0.005)	1.0	0.0724	>0.2
0.66	0.25	0.005	1.1		
0.67	0.26	0.004	1.0		
0.05 (0.001–0.86)	0.16 (0.06–0.72)	0.018 (0.001–0.13)	13.9	0.064	
0.03 (0.02–0.04)	0.35 (0.32–0.40)	0.019 (0.015–0.025)	23.1	0.010	0.021
0.05 (0.05–0.05)	0.34	0.020	13.9	0.025	
0.04	0.28	0.019	16.9		
0.05	0.34	0.018	13.9		
0.29 (0.14–0.42)	0.34 (0.27–0.40)	0.026 (0.017–0.035)	6.4 (3.0–9.8)		
0.16	0.33	0.020	4.3		

Also, the average time, T_h, to reduce virus infectivity to its mid-value, $(\beta_0 + \beta_\infty)/2$, given by $\ln(2)/k$, is 6.4 (95% CI = 3.0 to 9.8; median, 4.3) days (Table 1).

In Fig. 4 we show the change of infection rate $\beta(t)$ over time for all animals (black), donor animals (red), ramp-up plasma recipient animals (blue), and set-point plasma recipient animals (green). The corresponding horizontal dashed lines indicate the constant infection rate estimated using the model with constant infectivity. One can clearly see that for each group of animals, the time-dependent infection rate is very different from the constant infection rate predicted by the model with constant infectivity.

Comparison of ramp-up and set-point plasma recipient animals. The key parameters related to the time-dependent infectivity are the initial infection rate (β_0), the set-point infection rate (β_∞), and the exponential decay rate (k) of the infection rate. All of these parameters are higher in ramp-up plasma recipient animals than in set-point plasma recipient animals. The higher initial infection rate in ramp-up plasma recipient animals (6.0×10^{-8} ml RNA^{-1} day^{-1}) compared to the set-point plasma recipient animals (2.4×10^{-8} ml RNA^{-1} day^{-1}) shows that ramp-up plasma virus is more infectious than set-point plasma virus as suggested by the experiments (26).

Interestingly, the ramp-up plasma virus has a higher infectivity from the time of challenge to the set-point stage (Fig. 4). The infection rate decays much more rapidly in ramp-up plasma recipient animals ($k = 0.66$ day^{-1}), taking just 1.1 day to reach the mid-value $(\beta_0 + \beta_\infty)/2$, than in set-point plasma recipient animals (0.04 day^{-1}), taking 16.9 days to reach the mid-value. However, the infectivity in the set-point plasma recipients continues to decay for much longer, such that the ratio of β_0 to β_∞ is larger in set-point plasma recipient animals (~7) than in ramp-up plasma recipient animals (~3).

Cell death rate. The average value of the estimated infected cell loss rate δ is 0.34 (95% CI = 0.27 to 0.40; median, 0.33) day^{-1}. This value is consistent with the slow decay of SIV RNA from its peak observed in most animals (Fig. 2 and 3). We note that some other studies of primary infection have inferred higher mean values of δ (7, 33), although different virus strains and/or monkey species were used. Moreover, Nowak et al. (33) observed a large variation in the decay rates, encompassing, at the lower end, the values we estimate. Here we found d = 0.026 (95% CI = 0.017 to 0.035) day^{-1}, which is only slightly larger than the value estimated for humans (44).

Sensitivity analysis. Due to lack of information about the actual number of virions that initiate infection when virus is introduced intravaginally, we fit the viral load data in donor animals first assuming $V_0 = 1/300$ virions/ml and then by taking V_0 as 10- and 100-fold higher. With an increased V_0, we obtained lower estimates of T_0, β_0, k, and higher estimates of β_∞, whereas estimates of δ and d were not as sensitive to changes in V_0. For example, when V_0 is increased by 10-fold, the estimates of all parameters changed by less than 10% on average (Tables 3 and 4).

DISCUSSION

Prior models of acute HIV/SIV infection have assumed that the rate of target cell infection, β, is constant (33, 36, 44). The finding by Ma et al. (26) that plasma virus collected during

TABLE 2. Constant infectivity model: estimated parameter values[a]

Animal group[b]	T_0 (cells/μl)	$\bar{\beta}$ (10^{-8} ml/RNA/day)	δ (1/day)	d (1/day)	SSR
Group 1					
25479	131.4 (65.7–557.7)	1.18 (0.32–2.62)	0.19 (0.05–0.43)	0.03 (0.007–0.08)	0.176
25948	14.9 (5.4–37.3)	9.80 (4.35–28.67)	0.25 (0.21–0.33)	0.002 (0.001–0.003)	0.159
29459	139.1 (119.6–169.5)	1.10 (0.93–1.29)	0.35 (0.30–0.36)	0.018 (0.018–0.022)	0.030
29271	101.2 (77.5–138.3)	1.62 (1.24–2.17)	0.20 (0.19–0.22)	0.001 (0.001–0.002)	0.028
27361	10.5 (6.6–14.4)	15.63 (11.33–23.77)	0.12 (0.11–0.14)	0.002 (0.001–0.003)	0.099
29029	43.1 (32.0–63.2)	3.61 (2.49–4.73)	0.18 (0.15–0.24)	0.009 (0.007–0.015)	0.022
26811	21.3 (11.1–45.2)	4.24 (1.60–6.20)	0.20 (0.09–0.29)	0.008 (0.003–0.029)	1.141
25908	14.1 (7.6–28.0)	9.81 (5.1–17.7)	0.21 (0.15–0.26)	0.003 (0.002–0.004)	0.095
Mean	59.4	5.87	0.21	0.009	
Median	32.2	3.92	0.20	0.005	
Group 2					
35036	88.9 (29.1–846.7)	2.12 (0.19–5.43)	0.22 (0.13–0.33)	0.002 (0.001–0.003)	0.497
33815	40.3 (19.7–88.4)	3.29 (1.37–6.03)	0.19 (0.11–0.29)	0.009 (0.004–0.014)	0.185
36068	24.2 (2.6–53.8)	4.95 (2.04–41.80)	0.27 (0.18–0.41)	0.002 (0.001–0.004)	0.163
Mean	51.1	3.45	0.23	0.004	
Median	40.3	3.29	0.22	0.002	
Group 3					
34373	64.8 (26.4–264.6)	1.96 (0.62–4.05)	0.30 (0.06–1.47)	0.061 (0.001–0.21)	0.095
33952	37.2 (17.4–80.0)	3.45 (1.50–6.63)	0.25 (0.17–0.41)	0.007 (0.003–0.011)	0.134
34846	19.5 (19.5–19.5)	4.47 (4.47–4.47)	0.23 (0.23–0.23)	0.007 (0.007–0.007)	0.047
Mean	40.5	3.29	0.26	0.025	
Median	37.2	3.45	0.25	0.007	
Overall mean	53.6 (30.39–76.8)	4.80 (2.62–6.98)	0.23 (0.20–0.25)	0.011 (0.003–0.020)	
Overall median	38.7	3.53	0.22	0.007	

[a] The estimated parameter values T_0, $\bar{\beta}$ (constant infection rate), δ, d, and sum of squared residuals (SSR) for the eight donor animals, three ramp-up plasma recipient animals, and three set-point plasma recipient animals are indicated (26). Numbers in parentheses indicate the 95% CI.
[b] See Table 1, footnote *b*.

early infection has a greater ability to infect macaques compared to plasma virus collected in later stages suggests a temporal variation of virus infectivity. Moreover, preliminary data from HIV-1-infected patients comparing the ratio of 50% tissue culture infectious dose ($TCID_{50}$) with HIV RNA copy number has also suggested a decay of virus infectivity over time during primary infection (David Montefiori, unpublished data). These observations suggest that incorporating time-dependent infectivity into viral dynamics models might give rise to more realistic models and better parameter estimates and model predictions.

We thus introduced a viral dynamic model in which the rate of viral infection of $CD4^+$ T cells varies over time. The infection rate in our model decays exponentially from an initial high infectious level to a lower infectious level at set-point. We note that only limited data on primary infection exist and so there could be other forms of time-dependent infectivity, which can reasonably explain the data. Also, virus infectivity could continue to change after the set-point is reached. More data and more extensive studies are needed to provide a more accurate functional form mimicking the time dependency of virus infectivity during primary SIV/HIV-1 infection. However, we find that the model using infectivity in the form of exponential decay can explain the data reasonably and serves well to study the effect of time-dependent infectivity on viral dynamics. Inclusion of the temporal variation of virus infectivity made the model more closely mimic the measured viral dynamics since it gave rise to statistically significant better fits to the viral load data in more than 70% of the SIV-infected animals analyzed.

Although our model assumes that virus loses infectivity with time, there are other mechanistic explanations that might also be consistent with the viral load data. In the basic viral dynamic model it is very difficult to separate out the effects of a change in the infection rate, β, from a change in the infected cell virion production rate, p. For example, if β is decreased fewer cells are infected per unit time. However, the effect on viral kinetics can be mimicked by having β remain constant but having each infected cell produce less virus. As suggested by the work of Levy and others, $CD8^+$ T cells may secrete factors that reduce viral replication by infected cells (17, 23, 28), effectively reducing p. However, since these factors act on infected $CD4^+$ T cells, it seems unlikely that enough factors would be transferred in the experiments by Ma et al. (26) to explain the change in infectivity between ramp-up and set-point plasma. Cytolytic T-cell responses could also influence early viral kinetics as suggested by the rapidity at which viral escape variants are found (14, 40). However, viral escape should look like an increase in infectivity not a decrease. Clearly, antibody or other plasma factors could bind to virions and affect their infectivity, as already suggested (26).

Ma et al. (26) found that a 1-ml aliquot of diluted ramp-up plasma containing 2 vRNA copies could not infect naive macaques but that the same plasma diluted to 20 vRNA copies led to the infection of the three macaques tested. On the other hand, the set-point plasma diluted to 150 vRNA did not infect any of the three macaques tested, but a dilution to 1,500 vRNA successfully infected all three animals; 1,500 vRNA copies per ml was thus taken as a threshold for successful infection and

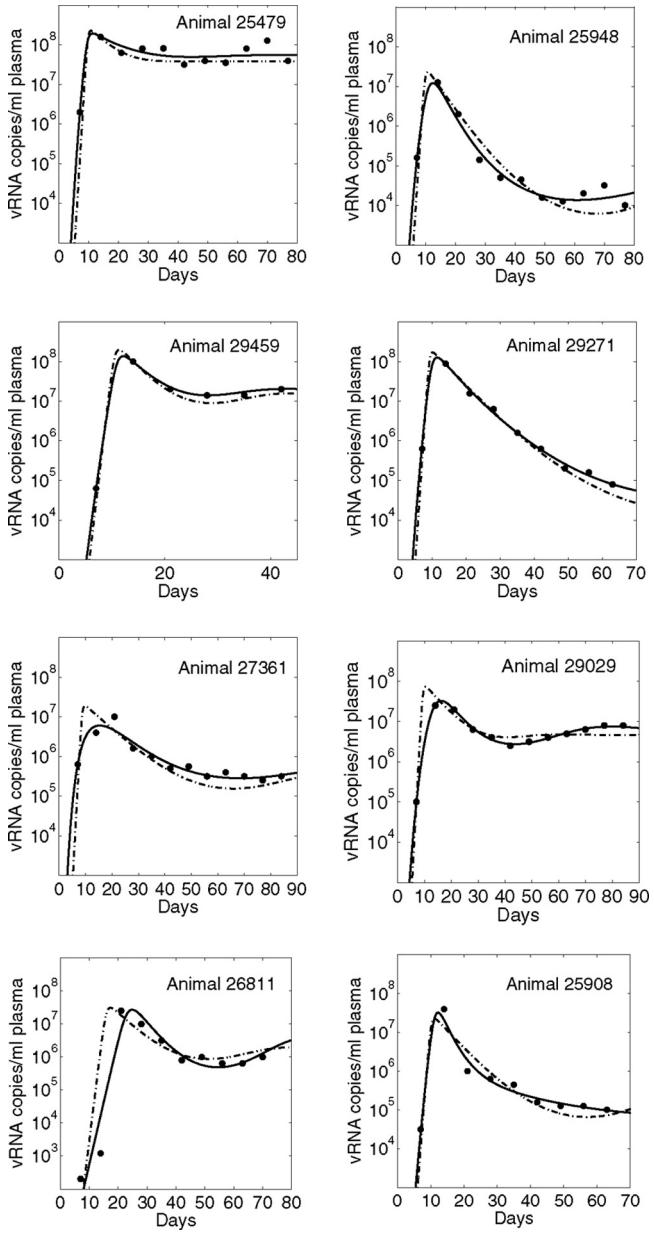

FIG. 2. Fitted viral dynamics curves using the two models (solid line, model with time-varying infectivity; dashed line, model with constant infectivity) to the observed viral load data (●) for the eight donor animals in reference 26. Note how the fits with the varying infectivity model are systematically better, especially during the early part of viral growth, when the infectivity is varying faster.

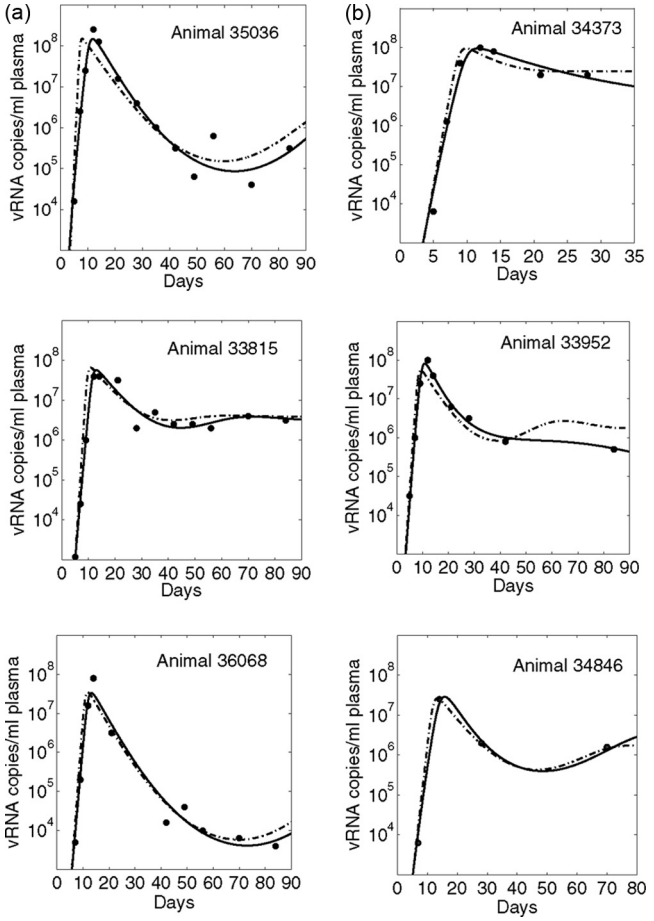

FIG. 3. Viral dynamics model curves using estimated parameters (solid line, model with time-varying infectivity; dashed line, model with constant infectivity) and observed viral load data (●) for three ramp-up plasma recipient animals (a) and three set-point plasma recipient animals in reference 26 (b).

information about set-point plasma between 150 and 1,500 copies per ml is not available. According to our model estimates, the initial infection rate, β_0, is higher in ramp-up plasma recipient animals than in set-point plasma recipients in agreement with the findings that ramp-up plasma is more infectious than set-point plasma (26). The fact that 20 vRNA copies from ramp-up plasma could initiate infection is surprising given that prior studies have found that fewer than 0.1% of virions in plasma or culture media are infectious (5, 22, 30, 42). However, a recent study (38) found that rapid dissociation of HIV-1 from cultured cells severely limits infectivity assays and masks the inherent high infectivity of virions.

By fitting our model to viral kinetic data we are estimating the infection rate β and not the number of infectious viruses in

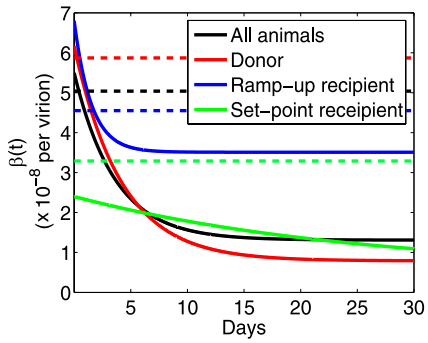

FIG. 4. Average time-varying infection rate $\beta(t)$ for donor animals (red), ramp-up plasma recipient animals (blue), set-point plasma recipient animals (green), and overall animals (black). Horizontal dashed lines represent the constant infection rate estimated by using model with constant infectivity.

TABLE 3. Estimated T_0, β_0, β_∞, k, δ, and d parameter values[a]

Animal	V_0 (RNA copies/ 300 ml)	T_0 (cells/μl)	β (10^{-8} ml/ RNA/day)		k (1/day)	δ (1/day)	d (1/day)
			β_0	β_∞			
25479	10	109.8	2.08	0.17	0.12	0.15	0.055
	100	98.8	1.90	0.18	0.11	0.15	0.055
25948	10	19.6	12.27	1.46	0.15	0.55	0.046
	100	18.9	10.57	1.48	0.13	0.53	0.045
29459	10	98.3	1.72	0.89	0.14	0.35	0.036
	100	96.6	1.43	0.93	0.09	0.36	0.039
29271	10	91.5	2.38	0.19	0.11	0.28	0.018
	100	88.5	2.00	0.21	0.10	0.28	0.018
27361	10	32.4	11.1	0.72	0.31	0.43	0.035
	100	29.4	10.1	0.75	0.29	0.41	0.036
29029	10	59.2	3.86	0.47	0.18	0.39	0.054
	100	44.8	3.51	0.57	0.12	0.31	0.046
26811	10	29.2	7.05	1.88	0.65	0.31	0.015
	100	26.6	5.45	1.92	0.58	0.30	0.016
25908	10	36.2	4.82	0.77	0.06	0.62	0.045
	100	35.2	4.42	0.82	0.05	0.63	0.043

[a] Shown are values for the eight donor animals in reference 26 for $V_0 = 10$ and 100 RNA copies/300 ml.

TABLE 4. Percent change in estimated parameters due to 10- and 100-fold increases in the initial viral load V_0 for the fits in Table 3

Parameter	% Change in V_0 (range) due to:	
	10-fold increase in V_0	100-fold increase in V_0
T_0	–7.5 (−3.9 to −11.0)	–14.8 (−7.4 to −30.8)
β_0	–8.3 (−2.5 to −13.5)	–20.2 (−15.3 to −33.1)
β_∞	+4.9 (0.0 to −11.8)	+12.4 (+5.0 to +32.6)
k	–9.7 (−6.3 to −14.3)	–24.7 (−14.7 to −43.8)
δ	–2.2 (−11.8 to +3.7)	–5.5 (−24.4 to +5.9)
d	+4.7 (−4.3 to +16.7)	+4.6 (−14.8 to +25.8)

an inoculum. We recognize that the probability of infection is not the same as the infectivity of free virus, and thus a direct comparison of the ratio of infectivities in ramp-up and set-point plasma from our model with the experimental results on the inoculum size needed for infection is not possible. Still, with small inocula, the probability of infection could be described by a stochastic model. In such a model the probability that a virion infects a cell before being cleared will play a role and thus the infectivity rate of a virion, β, can be tied to the probability of infection (46; J. E. Pearson, P. Krapivsky, and A. S. Perelson, unpublished result).

Assuming that the infection rate of $CD4^+$ T cells by SIV, β, decreases over the course of infection, as suggested by our modeling and data fitting, we made a number of interesting observations. First, we found that the estimated β_0 in the donor animals, which characterizes viral growth during their ramp-up phase, is similar to the estimated β_0 in the recipients of ramp-up plasma. Second, we found that the rate of decrease in infectivity varies between different groups of animals showing that this decay depends on the source of virus. The decay rate of infectivity was much slower in set-point plasma recipient animals (0.04 day^{-1}) than in ramp-up plasma recipients (0.66 day^{-1}). Even though the decay of infectivity is very slow in set-point plasma recipients, we still observe decay, suggesting that decay can occur past set-point. Our estimate of β_∞ in the ramp-up recipients is much higher than in the other two groups, donors and set-point recipients, for which β_∞ is similar (Table 1 and Fig. 4). Why this is the case is unknown but will likely need further experiments, for example, using the set-point plasma of ramp-up recipients to infect naive macaques and analyze the decay of infectivity in these. It may be that decay continues to occur past set-point and hence β_∞ was underestimated in the experiments using ramp-up plasma. In support of this, we note the ramp-up recipients were only monitored for 12 weeks, whereas the donor animals were monitored for 17 weeks, at which point the set-point plasma was collected. It may also be that the decay of infectivity is not a simple exponential and that to describe decay at longer times a more complex function is needed.

Although our model cannot conclusively address the mechanistic causes of the decay in infectivity, it is still interesting to speculate on what we can learn from these results about the potential explanations for the difference in infectivity of the virus at different stages of infection. Note that the infectivity of virus from donors at set-point ($\beta_\infty = 0.8 \times 10^{-8}$ ml RNA^{-1} day^{-1}) increases to $\beta_0 = 2.4 \times 10^{-8}$ ml RNA^{-1} day^{-1} in the recipients of this plasma. This may indicate that some process of elimination of less-infectious virus is occurring during the early stages of infection. Due to the rapid expansion of virus during ramp-up, low infectivity and hence slow-growing virus may simply get diluted out of the viral quasi-species. That is, the higher infectivity observed during the acute phase of infection may reflect the return of the virus population to optimal fitness, prior to the onset of immune selection, in a new host genetic background. Another possible explanation is that a plasma factor, such as antibody, is present in the set-point plasma and bound to this virus when in the donor animal. When the virus is transferred into a recipient animal and some virus in the inoculum successfully infects the recipient, new virus is made, which may be identical to that which infected the animal but which appears to be more infectious since there is no or little anti-SIV antibody or other antiviral factor present yet in the recipient animal. Hence, the β_0 in the recipients would be higher than the β_∞ in the donor. By the time set-point is reached antiviral plasma factors could be present, driven by the engagement of the immune response, and the value of infectivity may be similar in donors and set-point plasma recipients. Depending on the animal, the generation of these factors could continue, and infectivity could continue to decrease.

Similar observations of time-dependent virus infectivity have also been reported in hepatitis C virus (HCV) and hepatitis B virus (HBV) infections (1, 16, 18, 20, 45). The basis of the decline in infectivity for these viruses also still remains to be explained. However, as we show here, mathematical modeling can quantify these effects and may help in reaching an understanding of these early events in infection.

Even if we do not understand the molecular and cellular basis for decreases in infectivity of viruses during the course of infection, the fact that virus may be more infectious during acute infection than in later stages can have profound implications for the epidemiology of these infections. Already, individuals with acute HIV infection have been considered to be significant spreaders of infection due to the high viral loads attained during this period (21, 37, 48). If the infectivity of the virus is also increased during acute

infection, compared to chronic infection, then there could be a double-whammy effect where both more virus and more infectious virus contribute to the spread of HIV by acutely infected individuals. This may not have been fully appreciated before.

ACKNOWLEDGMENTS

Portions of this study were done under the auspices of the U.S. Department of Energy under contract DE-AC52-06NA25396 and supported by the Center for HIV/AIDS Vaccine Immunology, NIH grants AI28433-19 and RR06555-18 (A.S.P.), P20-RR18754 (R.M.R. and A.S.P.), and U51-RR00169 and P01 AI066314 (C.J.M.), as well as a gift from the James B. Pendleton Charitable Trust (C.J.M.).

REFERENCES

1. **Alter, H. J., R. Sanchez-Pescador, M. S. Urdea, J. C. Wilber, R. J. Lagier, A. M. Di Bisceglie, J. W. Shih, and P. D. Neuwald.** 1995. Evaluation of branched DNA signal amplification for the detection of hepatitis C virus RNA. J. Viral Hepat. **2:**121–132.
2. **Althaus, C. L., and R. De Boer.** 2008. Dynamics of immune escape during HIV/SIV infection. PLoS Comput. Biol. **4:**e1000103.
3. **Balamurugan, A., M. J. Lewis, C. M. R. Kitchen, et al.** 2008. Primary human immunodeficiency virus type 1 (HIV-1) infection during HIV-1 gag vaccination. J. Virol. **82:**2784–2791.
4. **Bates, D. M., and D. G. Watts.** 2007. Nonlinear regression analysis and its applications. John Wiley & Sons, Inc., Hoboken, NJ.
5. **Bourinbaiar, A. S.** 1994. The ratio of defective HIV-1 particles to replication-competent infectious virions. Acta Virol. **38:**59–61.
6. **Burg, D., L. Rong, A. Neumann, and H. Dahari.** 2009. Mathematical modeling of viral kinetics under immune control during primary HIV-1 infection. J. Theor. Biol. **259:**751–759.
7. **Chen, H. Y., M. Di Mascio, A. S. Perelson, D. D. Ho, and L. Zhang.** 2007. Determination of virus burst size *in vivo* using a single-cycle SIV in rhesus macaques. Proc. Natl. Acad. Sci. U. S. A. **104:**19079–19098.
8. **Ciupe, M. S., B. L. Bivort, D. M. Bortz, and P. W. Nelson.** 2006. Estimating kinetic parameters from HIV primary infection data through the eyes of three different mathematical models. Math. Biosci. **200:**1–27.
9. **Daar, E. S., T. Moudgil, R. D. Meyer, and D. D. Ho.** 1991. Transient high levels of viremia in patients with primary human immunodeficiency virus type 1. N. Engl. J. Med. **324:**916–964.
10. **De Boer, R., and A. S. Perelson.** 1998. Target cell limited and immune control models of HIV infection: a comparison. J. Theor. Biol. **190:**201–214.
11. **Efron, B., and R. Tibshirani.** 1986. Bootstrap methods for standard errors, confidence intervals, and other measures of statistical accuracy. Stat. Sci. **1:**54–75.
12. **Fiebig, E. W., D. J. Wright, B. D. Rawal, P. E. Garrett, R. T. Schumacher, L. Peddada, C. Heldebrant, R. Smith, A. Conrad, S. H. Kleinman, and M. P. Busch.** 2003. Dynamics of HIV viremia and antibody seroconversion in plasma donors: implications for diagnosis and staging of primary HIV infection. AIDS **17:**1871–1879.
13. **Fox, J., J. Weber, and S. Fidler.** 2006. Primary HIV. Sex. Transm. Infect. **82:**267–268.
14. **Goonetilleke, N., M. K. P. Liu, J. F. Salazar-Gonzelez, G. Ferrari, E. Giorgi, V. Ganusov, B. F. Keele, G. H. Learn, E. L. Turnbull, M. G. Salazar, K. J. Weinhold, S. Moore, B. N. Letvin, B. F. Haynes, M. S. Cohen, P. Hraber, T. Bhattacharya, P. Borrow, A. S. Perelson, B. H. Hahn, G. M. Shaw, B. T. Korber, A. J. McMichael, et al.** 2009. The first T-cell response to transmitted/founder virus contributes to the control of acute viremia in HIV-1 infection. J. Exp. Med. **206:**1252–1272.
15. **Haaft, P., N. Almond, G. Biberfeld, A. Cafaro, M. Cranage, B. Ensoli, G. Hunsmann, N. Polyanskaya, C. Stahl-Hennig, R. Thortensson, F. Titti, and J. Heeney.** 2001. Comparison of early plasma RNA loads in different macaque species and the impact of different routes of exposure on SIV/SHIV infection. J. Med. Prematol. **30:**207–214.
16. **Hijikata, M., Y. K. Shimizu, H. Kato, A. Iwamoto, J. W. Shih, H. J. Alter, R. H. Purcell, and H. Yoshikura.** 1993. Equilibrium centrifugation studies of hepatitis C virus: evidence for circulating immune complexes. J. Virol. **67:**1953–1958.
17. **Jin, X., D. E. Bauer, S. E. Tuttleton, S. Lewin, A. Gettie, J. Blanchard, C. E. Irwin, J. T. Safrit, J. Mittler, L. Weinberger, L. Kostrikis, L. Zhang, A. S. Perelson, and D. D. Ho.** 1999. Dramatic rise in plasma viremia after $CD8^+$ T-cell depletion in simian immunodeficiency virus infected macaques. J. Exp. Med. **189:**991–998.
18. **Katayama, K., J. Kumagai, Y. Komiyo, M. Mizui, H. Yugi, S. Kishimoto, R. Yamanaka, S. Tamatsukuri, T. Tomoguri, Y. Miyakawa, J. Tanaka, and H. Yoshizawa.** 2004. Titration of hepatitis C virus in chimpanzees for determining the copy number required for transmission. Intervirology **47:**57–64.
19. **Keele, B. F., H. Li, G. H. Learn, P. Hraber, et al.** 2009. Low-dose rectal inoculation of rhesus macaques by SIVsmE660 or SIVmac251 recapitulates human mucosal infection by HIV-1. J. Exp. Med. **206:**1117–1134.
20. **Komiya, Y., K. Katayama, H. Yugi, M. Mizui, H. Matsukura, T. Tomoguri, Y. Miyakawa, A. Tabuchi, J. Tanaka, and H. Yoshizawa.** 2008. Minimum infectious dose of hepatitis B virus in chimpanzees and difference in the dynamics of viremia between genotype A and genotype C. Transfusion **48:**286–294.
21. **Koopman, J. S., J. A. Jacquez, G. W. Welch, C. P. Simon, B. Foxman, S. M. Pollock, D. Barth-Jones, A. L. Adams, and K. Lange.** 1997. The role of early HIV infection in the spread of HIV through populations. J. Acquir. Immune Defic. Syndr. Hum. Retrovir. **14:**249–258.
22. **Kwon, Y. J., G. Hung, W. E. Anderson, C. A. Peng, and H. Yu.** 2003. Determination of infectious retrovirus concentration from colony-forming assay with quantitative analysis. J. Virol. **77:**5712–5720.
23. **Levy, J. A., C. E. Mackewicz, and E. Barker.** 1996. Controlling HIV pathogenesis: the role of noncytotoxic anti-HIV activity of CD8 cells. Immunol. Today **17:**217–224.
24. **Li, Q., L. Duan, J. D. Estes, Z. M. Ma, T. Rourke, Y. Wang, C. Reilly, J. Carlis, C. J. Miller, and A. T. Haase.** 2005. Peak SIV replication in resting memory $CD4^+$ T cells depletes gut lamina propria $CD4^+$ T cells. Nature **434:**1148–1152.
25. **Little, S. J., A. R. McLean, C. A. Spina, D. D. Richman, and D. V. Havlir.** 1999. Viral dynamics of acute HIV-1 infection. J. Exp. Med. **190:**141–150.
26. **Ma, Z., M. Stone, M. Piatak, B. Schweighardt, N. L. Haigwood, D. Montefiori, J. D. Lifson, M. Busch, and C. J. Miller.** 2009. High specific infectivity of plasma virus from the pre-ramp and ramp up stages of acute simian immunodeficiency virus infection. J. Virol. **83:**3288–3297.
27. **Macey, R. I., and G. F. Oster.** 2001. Berkeley Madonna, version 8.0. University of California at Berkeley, Berkeley, CA.
28. **Mackewicz, C. E., B. K. Patterson, S. A. Lee, and J. A. Levy.** 2000. $CD8^+$ cell noncytotoxic anti-human immunodeficiency virus response inhibits expression of viral RNA but not reverse transcription or provirus integration. J. General Virol. **81:**1261–1264.
29. **Markowitz, M., M. Louie, A. Hurley, E. Sun, M. Di Mascio, A. S. Perelson, and D. D. Ho.** 2003. A novel antiviral intervention results in more accurate assessment of human immunodeficiency virus type 1 replication dynamics and T-cell decay in vivo. J. Virol. **77:**5037–5038.
30. **Marozsan, A. J., E. Fraundorf, A. Abraha, H. Baird, D. Moore, R. Troyer, I. Nankja, and E. J. Arts.** 2004. Relationships between infectious titer, capsid protein levels, and reverse transcriptase activities of diverse human immunodeficiency virus type 1 isolates. J. Virol. **78:**11130–11141.
31. **Miller, C. J., Q. Li, K. Abel, E. Y. Kim, Z. M. Ma, S. Wietgrefe, L. La Franco-Scheuch, L. Compton, L. Duan, M. D. Shore, M. Zupancic, M. Busch, J. Carlis, S. Wolinsky, and A. T. Haase.** 2005. Propagation and dissemination of infection after vaginal transmission of simian immunodeficiency virus. J. Virol. **79:**9217–9227.
32. **Murray, J. M., G. Kaufmann, A. D. Kelleher, and D. A. Cooper.** 1998. A model of primary HIV-1 infection. Math. Biosci. **154:**57–85.
33. **Nowak, M. A., A. L. Lloyd, G. M. Vasquez, et al.** 1997. Viral dynamics of primary viremia and antiretroviral therapy in simian immunodeficiency virus infection. J. Virol. **71:**7518–7525.
34. **Perelson, A. S., P. Essunger, Y. Cao, M. Vesanen, A. Hurley, K. Saksela, M. Markowitz, and D. D. Ho.** 1997. Decay characteristics of HIV-1-infected compartments during combination therapy. Nature **387:**188–191.
35. **Perelson, A. S., and P. W. Nelson.** 1999. Mathematical analysis of HIV-1 dynamics of vivo. SIAM Rev. **41:**3–44.
36. **Phillips, A. N.** 1996. Reduction of HIV concentration during acute infection: independence from a specific immune response. Science **271:**497–499.
37. **Pilcher, C. D., H. C. Tien, J. J. Eron, et al.** 2004. Brief but efficient: acute HIV infection and the sexual transmission of HIV. J. Infect. Dis. **189:**1785–1792.
38. **Platt, E. J., S. L. Kozak, J. P. Durnin, T. J. Hope, and D. Kabat.** 2010. Rapid dissociation of HIV-1 from cultured cells severely limits infectivity assays, causes the inactivation ascribed to entry inhibitors, and masks the inherently high infectivity of virions. J. Virol. **84:**3106–3110.
39. **Pope, M., and A. T. Haase.** 2003. Transmission, acute HIV-1 infection and the quest for strategies to prevent infection. Nat. Med. **9:**847–852.
40. **Price, D. A., P. J. R. Goulder, P. Klenerman, A. K. Sewell, P. J. Easter-brook, M. Troop, C. R. M. Bangham, and R. E. Phillips.** 1997. Positive selection of HIV-1 cytotoxic T lymphocyte escape variants during primary infection. Proc. Natl. Acad. Sci. U. S. A. **94:**1890–1895.
41. **Ramratnam, B., S. Bonhoeffer, J. Binley, A. Hurley, L. Zhang, J. E. Mittler, M. Markowitz, J. P. Moore, A. S. Perelson, and D. D. Ho.** 1999. Rapid production and clearance of HIV-1 and hepatitis C virus assessed by large volume plasma apheresis. Lancet **354:**1782–1785.
42. **Rusert, P., M. Fischer, B. Joos, C. Leemann, H. Kuster, M. Flepp, S. Bonhoeffer, H. F. Gunthard, and A. Trkola.** 2004. Quantification of infectious HIV-1 plasma viral load using a boosted in vitro infection protocol. Virology **326:**113–129.
43. **Schacker, T., A. Collier, J. Hughes, T. Shea, and L. Corey.** 1996. Clinical and epidemiologic features of primary HIV infection. Ann. Intern. Med. **125:**257–264.

44. **Stafford, M. A., L. Corey, Y. Cao, E. S. Daar, D. D. Ho, and A. S. Perelson.** 2000. Modeling plasma virus concentration during primary HIV infection. J. Theor. Biol. **203:**285–301.
45. **Tabuchi, A., J. Tanaka, K. Katayama, M. Mizui, H. Matsukura, H. Yugi, T. Shimada, Y. Miyakawa, and H. Yoshizawa.** 2008. Titration of hepatitis B virus infectivity in the sera of pre-acute and late acute phases of HBV infection: transmission experiments to chimeric mice with human liver repopulated hepatocytes. J. Med. Virol. **80:**2064–2068.
46. **Tuckwell, H. C., P. D. Shipman, and A. S. Perelson.** 2008. The probability of HIV infection in a new host and its reduction with microbicides. Math. Biosci. **214:**81–86.
47. **Veazey, R. S., and A. A. Lackner.** 2004. Getting to the guts of HIV pathogenesis. J. Exp. Med. **200:**697–700.
48. **Wawer, M. J., R. H. Gray, N. K. Sewankambo, D. Serwadda, X. Li, O. Laeyendecker, N. Kiwanuka, G. Kigozi, M. Kiddugavu, T. Lutalo, F. Nalugoda, F. Wabwire-Mangen, M. P. Meehan, and T. C. Quinn.** 2005. Rates of HIV-1 transmission per coital act, by stage of HIV-1 infection, in Rakai, Uganda. J. Infect. Dis. **191:**1403–1409.
49. **Zhang, L., P. J. Dailey, A. Gettie, J. Blanchard, and D. D. Ho.** 2002. The liver is a major organ for clearing simian immunodeficiency virus in rhesus monkeys. J. Virol. **76:**5271–5273.